ORIGINAL ARTICLE

European Journal of Applied Physics
www.ej-physics.org

Spin Interpreted as the Angular Momentum Curvature, Electron g-factor Interpreted as the Ratio of Toroidal Torsion and Curvature, Unlocking of the Fixed Planck Constant h – New Tests for Old Physics

Jiří Stávek

ABSTRACT

We have proposed several new rules for the description of events in the microworld. We have newly defined the interpretation of the quantum spin as the angular momentum curvature and defined the geometry of helixes and toroidal helixes of quantum particles. Some new properties of quantum particles can be experimentally tested. Based on this concept we have defined the electron g-factor as the ratio of the toroidal torsion and curvature and events between the electron and its coupling photon. From this model we have extracted the values of the fine-structure constant α and the Planck constant h. The comparison of these values with the latest experimental data reveals some possible circular arguments in the experimental determination – the so-called SI barrier created by the fixing of the SI constants (SI – International System of Units). We propose on the one side to analyze those possible circular arguments and on the other side to continue to develop new generations of instruments for getting one or two more significant figures of those values h and c. The predictions of this classical model could be compared with the best predictions of QED (quantum electrodynamics) for the fine-structure constant α.

Keywords: Curvature and torsion in the microworld, helixes and toroidal helixes, g-factor newly defined, unlocking the fixed Planck constant and the constant of the speed of light.

Published Online: February 17, 2021

ISSN: 2684-4451

DOI :10.24018/ejphysics.2021.3.1.50

Jiří Stávek*
Independent Researcher, Prague, Czech Republic.
(e-mail: stavek.jiri@seznam.cz)

****Corresponding Author***

I. Introduction

There are known many attempts to describe the events in the microworld by the classical physics or by the old quantum mechanics, e.g., [1]-[9]. All these ad-hoc models cannot compete with the mathematical description developed by the QM (quantum mechanics). We need to discover some new rules as our guides into the microworld.

We propose to interpret the quantum spin as the angular momentum curvature and the angular frequency as the angular torsion. Based on these simple concepts we can define the geometry of helixes and toroidal helixes of quantum particles. Some new properties of those quantum particles can be experimentally observed.

In order to present the potential of these models we have derived the electron g-factor as the ratio of toroidal torsion and curvature and interactions between the electron and its coupling photon. Based on this model we have extracted the value of the fine-structure constant α and compared it with the latest experimental data and QED value. We want to open a discussion about the SI barrier in the experiments determining the fine-structure constant α and the Planck constant h. We assume that some circular arguments might be hidden in those experimental techniques – the input data are based on the fixed SI constants and thus influence the output data. Therefore, we propose to analyze those possible circular arguments and further develop new experimental techniques in order to extract one or two more significant figures in the Planck constant h and the constant of the speed of light c.

II. Helixes and Toroidal Helixes

The key idea of this geometrical description is to define the spin as the angular momentum curvature and the angular frequency as the angular torsion for the helix:

$$\begin{aligned} x(t) &= a \times \cos(t) \\ y(t) &= a \times \sin(t) \\ z &= b \times t \end{aligned} \qquad (1)$$

The geometrical parameters of helixes are summarized in Table I where λ is the Compton wavelength for that quantum particle [λ_x=h/(mc)], κ is the curvature, and τ is the torsion of that helix, S stands for the spin of that helix – the angular momentum curvature:

$$S = \frac{m_x c}{\kappa} \qquad (2)$$

where m_x is the mass of a given quantum particle.

TABLE I: GEOMETRY OF HELIXES

Graviton	Photon	Electron	Proton	Neutron
$a=\frac{\lambda_g}{2\pi}$	$a=\frac{\lambda_f}{4\pi}$	$a=\frac{\lambda_e}{8\pi}$	$a=\frac{\lambda_p}{8\pi}$	$a=\frac{\lambda_n}{8\pi}$
$a=\frac{\lambda_g}{2\pi}$	$a=\frac{\lambda_f}{4\pi}$	$a=\frac{\lambda_e}{8\pi}$	$a=\frac{\lambda_p}{8\pi}$	$a=\frac{\lambda_n}{8\pi}$
$b=\frac{\lambda_g}{2\pi}$	$b=\frac{\lambda_f}{4\pi}$	$b=\frac{\lambda_e}{8\pi}$	$b=\frac{\lambda_p}{8\pi}$	$b=\frac{\lambda_n}{8\pi}$
$\kappa=\frac{\pi}{\lambda_g}$	$\kappa=\frac{2\pi}{\lambda_f}$	$\kappa=\frac{4\pi}{\lambda_e}$	$\kappa=\frac{4\pi}{\lambda_p}$	$\kappa=\frac{4\pi}{\lambda_n}$
$\tau=\frac{\pi}{\lambda_g}$	$\tau=\frac{2\pi}{\lambda_f}$	$\tau=\frac{4\pi}{\lambda_e}$	$\tau=\frac{4\pi}{\lambda_p}$	$\tau=\frac{4\pi}{\lambda_n}$
$S=\pm\frac{h}{\pi}$	$S=\pm\frac{h}{2\pi}$	$S=\pm\frac{h}{4\pi}$	$S=\pm\frac{h}{4\pi}$	$S=\pm\frac{h}{4\pi}$

We might newly interpret the very well-known properties of quantum particles. E.g., the observed universal constant light speed c of photons can be interpreted as an interplay between the curvature and torsion of that helix:

$$c^2=\frac{c}{\kappa}\times c\tau \tag{3}$$

where the first term with curvature describes the amplitude of that helix and the second part with torsion describes the angular frequency of that helix. There are two typical situations – the first one was discovered by Albert Einstein as the special relativity [10] and the second one was discovered by Albert Einstein as the general relativity [11]. The elasticity of the spacetime was postulated in both Einstein´s theories. In this model we postulate the elasticity of the photon helix:

$$c^2=\frac{c}{\kappa}\times c\tau=\frac{c\lambda_f}{2\pi}\sqrt{\frac{1\pm\frac{v}{c}}{1\mp\frac{v}{c}}}\quad\frac{c\,2\pi}{\lambda_f}\sqrt{\frac{1\mp\frac{v}{c}}{1\pm\frac{v}{c}}} \tag{4}$$

$$c^2=\frac{c}{\kappa}\times c\tau=\frac{c\lambda_f}{2\pi}\sqrt{1-\frac{R_S}{R}}\quad\frac{c\,2\pi}{\lambda_f\sqrt{1-\frac{R_S}{R}}} \tag{5}$$

where R_S is the Schwarzschild radius and R the distance from the gravity source.

Under the influence of gravitons, photon helix is transformed at the distance R from the gravity source as:

$$\textit{photon helix}\rightleftarrows\textit{toroidal helix}$$
$$\frac{\tau}{\kappa}=1\quad\rightleftarrows\quad\frac{\tau}{\kappa}=2 \tag{6}$$

Therefore, we can interpret the Einstein´s and von Soldner´s deflections [12] of light by the Sun as:

$$\delta=\frac{4GM}{c^2R}=\frac{2GM}{c^2R}\frac{\tau}{\kappa}=\frac{2GM}{c^2R}2 \tag{7}$$

where G is the gravitational constant, M is the Sun mass, and R the radius of the Sun.

The photon helix is curved in the presence of the gravitational mass on the dependence of the distance R. At the distance R_S (the Schwarzschild radius), the photon helix circulates around the Schwarzschild black hole on the radius R_S and cannot escape.

TABLE II: GEOMETRY OF TOROIDAL HELIXES

Parameter	Electron	Proton	Neutron
Poloidal radius	$r=\frac{\lambda_e}{8\pi}$	$r=\frac{\lambda_p}{8\pi}$	$r=\frac{\lambda_n}{8\pi}$
Toroidal radius	$R=\frac{\lambda_e}{\pi}$	$R=\frac{2\lambda_p}{\pi}$	$R=\frac{2\lambda_n}{\pi}$
Zitterbewegung boundary - maximal	$R_{max}=\frac{9\lambda_e}{8\pi}$	$R_{max}=\frac{17\lambda_p}{8\pi}$	$R_{max}=\frac{17\lambda_n}{8\pi}$
Zitterbewegung boundary - minimal	$R_{min}=\frac{7\lambda_e}{8\pi}$	$R_{min}=\frac{15\lambda_p}{8\pi}$	$R_{min}=\frac{15\lambda_n}{8\pi}$
Annulus	$A=\frac{\lambda_e^2}{2\pi}$	$A=\frac{\lambda_p^2}{\pi}$	$A=\frac{\lambda_n^2}{\pi}$
Toroidal surface	$B=\frac{\lambda_e^2}{2}$	$B=\lambda_p^2$	$B=\lambda_n^2$
Toroidal volume	$V=\frac{\lambda_e^3}{32\pi}$	$V=\frac{\lambda_p^3}{16\pi}$	$V=\frac{\lambda_n^3}{16\pi}$
Circumference of toroid	$O=2\lambda_e$	$O=4\lambda_p$	$O=4\lambda_n$
Toroidal turns	$N=2$	$N=4$	$N=4$
Poloidal turns	$n=8$	$n=16$	$n=16$

Fig. 1 shows the geometry of the photon helix. There could be observed a new effect - the inner tunnel in the photon helix with the radius $r=\lambda_f/(4\pi)$. This tunnel could be found on the screen provided that photons fly directly from their source without any disturbance - no optical elements and no scattering along the path towards to the screen. The individual photons can create a joint self-organized pattern.

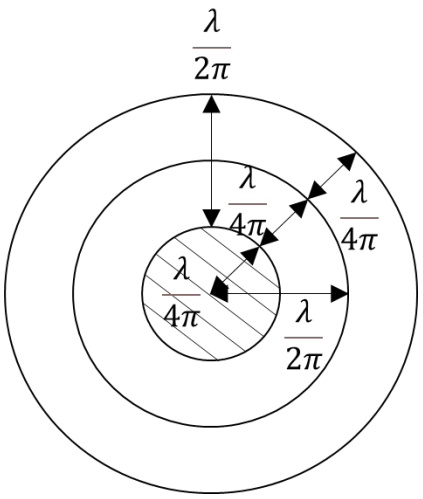

Fig. 1. Geometry of the photon helix – top view.

Electron, proton, and neutron form toroidal helixes with parameters summarized in Table II. Based on these parameters we can newly interpret several effects, e.g., the proton charge puzzle [13], where the experimental data oscillates around the proton toroidal radius in the range of the proton zitterbewegung.

Fig. 2 shows the geometry of the electron toroidal helix with the classical charge in the middle of this toroidal helix. The coupling photon oscillates between the toroidal helix and

European Journal of Applied Physics
www.ej-physics.org

the classical charge with radius r_e. This effect will be used for the evaluation of the electron g-factor.

When fermion is closed in the toroidal helix, then its "rest mass" energy is latent. If we will be able to transform the fermion toroidal helix into the helix in a controlled way, we might get an approach to the enormous source of sensible energy:

$$\begin{aligned} &\textit{latent energy} \rightarrow \textit{sensible energy} \\ &\textit{toroidal helix} \rightarrow \textit{helix} \\ &E_0 = 2m_e c^2 \rightarrow E = 2m_e c^2 = h\nu_e \end{aligned} \tag{8}$$

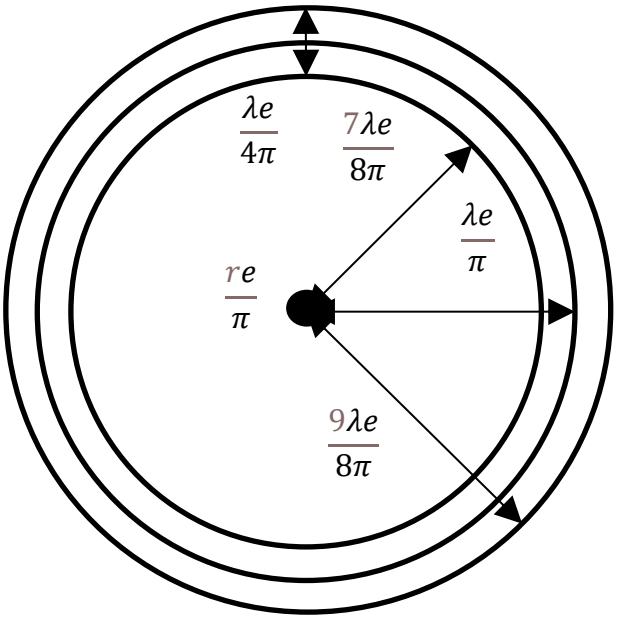

Fig. 2. Geometry of the electron toroidal helix.

III. ELECTRON G-FACTOR

We want to show the potential of this model and will try to describe the electron g-factor [14] as the ratio of the toroidal torsion and curvature and four interactions of the electron with its coupling photon:

$$\begin{aligned} -g_e &= S_0 + S_1\frac{\alpha}{\pi} + S_2\left(\frac{\alpha}{\pi}\right)^2 + \\ &+ S_3\left(\frac{\alpha}{\pi}\right)^3 + S_4\left(\frac{\alpha}{\pi}\right)^4 \end{aligned} \tag{9}$$

where the individual contributions to the electron g-factor are given in Table III.

The component S_0 describes the motion of the electron on the toroidal helix guided by the curvature and torsion of that toroidal helix.

The fine-structure constant α [15] is interpreted here as the ratio of the circumference of the classical charge with the classical radius of electron r_e and the radius of the electron toroidal helix:

$$\alpha = \frac{2\pi\frac{r_e}{\pi}}{\frac{\lambda_e}{\pi}} = \frac{2\pi\, r_e}{\lambda_e} \Rightarrow \frac{\alpha}{\pi} = \frac{2\, r_e}{\lambda_e} \tag{10}$$

TABLE III: COMPONENTS OF THE ELECTRON G-FACTOR

Ratio of the toroidal torsion and curvature
$S_0 = \frac{\tau}{\kappa} = \text{cotan}(\theta) = +2$
Linear specular reflection of the coupling photon
$S_1 = +1$
Surface diffuse reflection of the coupling photon
$S_2 = -\frac{2}{\pi}$
Volume diffraction of the coupling photon
$S_3 = -J_1(x)\,\frac{16}{3}$
$J_1(x)$ =1.219669891266504...
Rayleigh criterion for diffraction
Absorption and emission of the coupling photon
$S_4 = +\frac{128}{3}$

The component S_1=+1 describes the specular reflection of the coupling photon between the classical electron charge and the toroidal helix.

The component S_2 describes the surface diffuse reflection of the coupling photon between the surface of the classical charge and the surface of the toroidal helix:

$$S_2 = -\frac{4\pi\left(\frac{r_e}{\pi}\right)^2}{\frac{\lambda_e^2}{2}} = -\frac{2}{\pi}\left(\frac{2r_e}{\lambda_e}\right)^2 = -\frac{2}{\pi}\left(\frac{\alpha}{\pi}\right)^2 \tag{11}$$

The component S_3 describes the volume diffraction of the coupling photon between the volume of the classical charge and the volume of the toroidal helix:

$$\begin{aligned} S_3 &= -J_1(x)\,\pi\frac{\frac{4\pi}{3}\left(\frac{r_e}{\pi}\right)^3}{\frac{\lambda_e^3}{32\pi}} = \\ &= -J_1(x)\,\frac{16}{3}\left(\frac{\alpha}{\pi}\right)^3 \end{aligned} \tag{12}$$

where the $J_1(x)$ is the Rayleigh criterion [16] for the diffraction.

The component S_4 describes the absorption and emission of the coupling photon between the classical charge and the toroidal helix. The dimensions were taken from the Einstein absorption and emission coefficients [17], the zitterbewegung of electron [18], [19] was described via the poloidal radius of the electron:

$$S_4 = \frac{2\pi\frac{r_e}{\pi}}{\frac{\lambda_e}{8\pi}} \times \frac{\frac{4}{3}\pi\left(\frac{r_e}{\pi}\right)^3}{\frac{\lambda_e^3}{32\pi}} = \frac{128}{3}\left(\frac{\alpha}{\pi}\right)^4 \tag{13}$$

We assume that these five components fully describe the g-factor of the electron. At this moment we will not work with additional adjustment and will work with this simple model with five components.

The electron g-factor is one of the best experimentally determined quantity in physics with 2018 CODATA recommended value [14] as:

European Journal of Applied Physics
www.ej-physics.org

$$g_e = -2.002\,319\,304\,362\,56(35)$$

Based on this presented model we can extract the fine-structure constant α_{ge} from (9) as:

$$\alpha_{ge}^{-1} = 137.035\,995\,837\,96(XX)$$

If we compare this value α with the latest experimental data, we see the difference in the ninth significant figure. We want to open discussion on a possible SI barrier in the evaluation of experimental observations while the input SI data might influence the final result.

IV. Fine-Structure Constant

The fine-structure constant α remains one of the most fascinating fundamental constants and continue to attract the attention of many physicists while it plays the central role in the physics by testing the most accurate theories such as quantum electrodynamics (QED). The constant α is also a keystone for the determination of other fundamental constants of the International System of units (SI).

The best experimental technique to determine the fine-structure constant α is based on the precise value of the ratio h/m_u – the ratio of the Planck constant and the atomic mass constant [20]-[23].

We have surveyed the events in the Ramsey-Bordé atom interferometer used for these experiments and have been proposing a working hypothesis about a possible SI barrier – in input data are somehow hidden SI h units that will reappear at the output of these experiments:

$$\alpha^2 \sim \omega_r \lambda_{eff}^2 \sim \nu_L \frac{1}{k_L^2} = \frac{E_L}{h_{SI}} \left(\frac{h_{SI}}{2\pi mc} \right)^2 \sim h_{SI} \qquad (14)$$

where ω_r is the measured recoil frequency, λ_{eff} is the effective wavelength, ν_L is the frequency of the used laser, k_L is the wavenumber of the used laser. We assume that via this channel the h_{SI} entered into the input data and then via this possible circular argument appeared at the output value as h_{SI}.

We propose to analyze this possible circular argument and to re-use other older techniques for the determination of the fine-structure constant in order to avoid this possible circular argument. The actual values of the fine-structure constant α are summarized in Table IV.

Table IV: Values of the Fine-Structure Constant

Determination	α^{-1}
This model	137.03599❺❽❸❼❾❻(XX)
QED [24]	137.03599❾❶❺❿(33)
CODATA [15]	137.03599❾❿❽❹(21)
Parker [21]	137.03599❾❿❹❻(27)
Morel [23]	137.03599❾❷❿❻(11)

V. The Fixed Planck Constant

The Planck constant h is the quantum of electromagnetic action that relates a photon´s energy to its frequency and plays the very important role in different fields of modern physics [25]. Since May 20, 2019 the numerical value of the Planck constant has been fixed, with finite significant figures [26]-[29]. The value h_{SI} was experimentally determined using two techniques: The Kibble balance [30]-[33], and the X-ray-crystal-density (XRCD) [34], [35].

These two independent experimental techniques are capable of realizing the definition of the kilogram with relative uncertainties within few parts in 10^8. Table V and Fig. 3 summarize the latest experimental values of the Planck constant together with the fixed SI value. We have added to this Table V and Fig. 3 the Planck value h_{ge} extracted from our model from the fine-structure constant given in Table V.

Table V: Values of the Planck Constant

$\mathbf{h_{SI}}$	6.6260❼❿❶❺❿(69)
NIST-17	6.6260❻❾❾❸❹(88)
NRC-17	6.6260❼❿❶❸❸(60)
$\mathbf{h_{KIBBLE}}$	6.6260❼❿❿❸❹
IAC-15	6.6260❼❿❷❷(13)
IAC-17	6.6260❼❿❹❿❺(77)
NMIJ-17	6.6260❼❿❶❸(16)
$\mathbf{h_{XRCD}}$	6.6260❼❿❷❺❷
This model	
$\mathbf{h_{ge}}$	6.6260❻❾❾❾❸❿(XX)

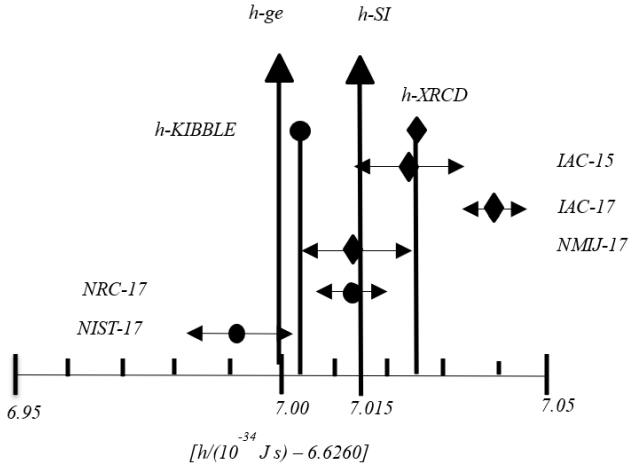

Fig. 3. Experimental values of the Planck constant with the SI fixed value.

VI. Two Possible Circular Arguments

We have tried to analyze the input data entering into these quantifications with the aim to discover a possible circular argument in those techniques because there is visible a minor difference between the value h_{KIBBLE} found by the Kibble balance and the value h_{XRCD} found by the X-ray-crystal-density method.

The experimental value h_{XRCD} is based on the formula:

$$\frac{h_{XRCD}}{m(Si)} = \frac{1}{2} \frac{A_r(e)}{A_r(Si)} \frac{\alpha^2 c}{R_\infty} \qquad (15)$$

where m(Si) is the mass of a single Si atom, $A_r(e)$ and $A_r(Si)$ are the relative atomic masses of electron and Si, α is the fine-structure constant, c is the speed of light, and R_∞ is the Rydberg constant. The experimental procedure is very impressive but in the final calculation the fine-structure constant α has to be inserted into the calculation. We assume that via this step the h_{SI} entered into the final result – see the

possible circular argument depicted in Fig. 4. We propose to re-analyze this procedure with the focus on the history of the determination of α. On the other side, we propose to further develop other techniques for the experimental determination of α.

The experimental value h_{KIBBLE} is based on the formula:

$$h_{KIBBLE} = \frac{m\, v_z\, g}{r\, f_1 f_2} \tag{16}$$

where m is the mass of a test mass, g the local gravitational acceleration, v_z the vertical velocity of the coil, r is the numerical value, f_1 and f_2 are the microwave frequencies, for details see [33].

The experimental procedure is very sophisticated, however, in this case the SI constant c_{SI} of the speed of light could entered as:

$$h_{KIBBLE} \sim \frac{1}{f_1 f_2} = \frac{c_{SI}^2}{\lambda_1 \lambda_2} \tag{17}$$

We assume that via this step the constant c_{SI} of the speed of light could penetrate into that calculation. Fig. 5 shows this possible circular argument.

If we are allowed to re-open the fixed value c_{SI} of the speed of light, we can achieve this result:

$$h_{ge} \approx h_{KIBBLE} \times \left(\frac{c_{SI}}{c_{ge}} \right)^2 = h_{KIBBLE} \times \left(\frac{299792458}{299792458.915} \right)^2$$

We know from the literature that the value for the speed of light was fixed in 1983 [36].

The last four experimental determinations of the speed of light are given in Table VI.

Table VI: THE EXPERIMENTAL VALUES OF THE SPEED OF LIGHT

1972 Evenson [37]	29979245**8**.**8**(1.2)(peak)
1973 CCDM	29979245**8**.**0**(1.2)
1974 Blaney [38]	29979245**9**.**0**(0.6)
1978 Woods [39]	29979245**8**.**8**(0.2)
1983 BIPM SI fixed	29979245**8**
2021	29979245**8**.**9**1**5**(XX)

We arrived to the conclusion that the experimental techniques for the determination of the electron g-factor, the fine-structure constant α, the Planck constant h, and the speed of the light c should be intensively promoted in order to obtain one or two more significant figures for each of them. We are now at the boundary where we can test our best physical model based on the QED theory and a possible new candidate based on the old quantum mechanics. The fixing of SI constants might mask the real effects [40].

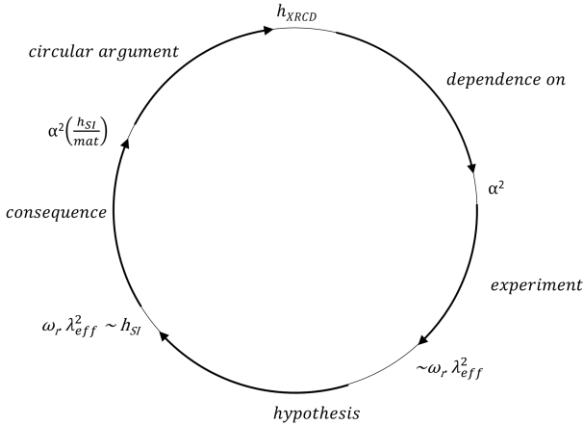

Fig. 4. A possible circular argument hidden in the X-ray-crystal density technique during the determination of the Planck constant.

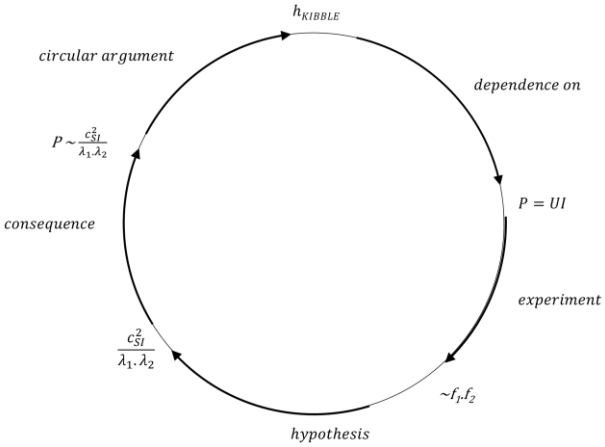

Fig. 5. A possible circular argument hidden in the Kibble balance technique during the determination of the Planck constant.

VII. CONCLUSION

A new model of the geometry of the microworld was presented. The model is based on helixes and toroidal helixes of quantum particles. There were proposed several new effects for the experimental evaluation. The most critical part is the interpretation of the electron g-factor that might add several significant figures to the fine-structure constant α, the Planck constant h, and the constant of the speed of light c.

ACKNOWLEDGMENT

We were supported by the contract number 0110/2020.

REFERENCES

[1] N. Bohr, "On the constitution of atoms and molecules," *Phil. Mag*., vol. 26, pp. 1- 24, 1913.
[2] A. L. Parson, "A magneton theory of the structure of the atom," *Smithsonian Miscellaneous Collection*, Pub. 2371, 80 pp, 1915.
[3] A. H. Compton, "The magnetic electron," *Journal of the Franklin Institute*, vol. 192, pp. 145-155, (1921).
[4] L. S. Lewitt, "Is the photon a double helix?" *Lett. Nuovo Cim*., vol. 21, pp. 222-223, 1978.
[5] J. G. Williamson, and M. B. van der Mark, "Is the electron a photon with toroidal topology?" *Annales de la Fondation Louis de Broglie*, vol. 22, pp. 133, (1997).
[6] M. H. Mac Gregor, *The enigmatic electron*, 2nd edition, El Mac Books, USA, 2013.
[7] O. Consa, "Helical model of the electron," *Progress in Physics*, vol. 14, pp. 80-90, 2018.

[8] R. Gauthier, "Quantum-entangled superluminal double-helix photon produces a relativistic superluminal quantum-vortex zitterbewegung electron and positron," *J. Phys.: Conf. Ser.*, vol. 1251, 012016, 2019.
[9] S. Chen, "Double-helix structure of photon," *Physical Science International Journal*, vol. 24, no. 55532, 2020.
[10] A. Einstein, "Zur Elektrodynamik der bewegter Körper," *Annalen der Physik*, vol.17, pp. 891-921, 1905.
[11] A. Einstein, "Die Feldgleichungen der Gravitation," *Sitzungsberichte der Preussischen Akademie der Wissenschaften zu Berlin*, pp. 844-847, 1915.
[12] J. Soldner, "Űber die Ablenkung eines Lichtstrahls von seiner geradliniger Bewegung durch die Atraktion eines Weltkörpers, an welchem er nahe vorbeigeht," *Berliner Astronomisches Jahrbuch*, pp. 161-172, 1801.
[13] J. P. Karr, and D. Marchand, "Progress on the proton-radius puzzle," *Nature*, pp. 61-62, 2019.
[14] "*2018 CODATA Value: electron g factor*," The NIST Reference on Constants, Units, and Uncertainty. NIST, 20 May, 2019.
[15] P. J. Mohr, B. J. Taylor, and D. B. Newell, "Fine structure constant," *CODATA Internationally recommended 2018 values of the fundamental physical constants*, 2019.
[16] Lord Rayleigh, "Investigations in optics with special reference to the spectroscopy," *Philosophical Magazine*, vol. 8, pp. 261-274, 1879.
[17] A. Einstein, "Strahlungs-Emission und -Absorption nach der Quantentheorie," *Verhandlungen der Deutschen Physikalischen Gesselschaft*, vol. 18, 318-323, 1916.
[18] E. Schrödinger, "Zur Quantendynamik des Elektrons," In *Sitzungsberichte der Preussischen Akademie der Wissenschaften, Physikalisch-Mathematische Klasse*, pp. 63-72, 1931.
[19] D. Hestenes, "The zitterbewegung interpretation of quantum mechanics," *Foundations of Physik*, vol. 20, pp. 1213-1232, 1990.
[20] R. Bouchendira, P. Cladé, S. Guellati-Khélifa, F. Nez, and F. Biraben, "State of the art in the determination of the fine structure constant: test of Quantum Electrodynamics and determination of h/m_u," *Annalen der Physik*, pp. 1-9, 2018.
[21] R. H. Parker, Ch. Yu, W. Zhong, B. Estey, and H. Müller, "Measurement of the fine-structure constant as a test of the Standard Model", *Science*, vol. 360, pp. 191-195, 2018.
[22] P. Cladé, F. Nez, F. Biraben, and S. Guellati-Khélifa, "State of the art in the determination of the fine-structure constant and the ratio h/m_u," *Comptes Rendus Physique*, vol. 20, pp. 77-91, 2019.
[23] L. Morel, Z. Yao, P. Cladé, and S. Guellati-Khélifa, "Determination of the fine-structure constant with an accuracy of 81 perts per trillion," *Nature*, vol. 588, 61-65, 2020.
[24] T. Aoyama, T. Kinoshita, and M. Nio, "Revised and improved value of the QED tenth-order electron anomalous magnetic moment," *Physical Review D*, vol. 97, 036001, 2018.
[25] R. Steiner, "History and progress on accurate measurements of the Planck constant," *Rep. Prog. Phys.*, vol. 76, 016101, 2013.
[26] P. J. Mohr, D. B. Newell, B. N. Taylor, and E. Tiesinga, "Data and analysis for the CODATA 2017 special fundamental constants adjustment," *Metrologia*, vol. 55, pp. 125-146, 2018.
[27] D. B. Newell et al., "The CODATA 2017 values of *h*, *e*, *k*, and N_A for the revision of the SI," *Metrologia*, vol. 55, pp. L13-L16, 2018.
[28] Special Issue: The Revised SI: "Fundamental constants, basic physics and units," *Annalen der Physik*, vol. 531, Issue 5, 2019.
[29] M. A: Martin-Delgado, "The new SI and the fundamental constants of nature," *European Journal of Physics*, vol. 41, 063003, 2020.
[30] I. A. Robinson, and S. Schlamminger, "The watt or Kibble balance: a technique for implementing the new SI definition of the unit of mass," *Metrologia*, vol. 53, pp. A46-A74, 2016.
[31] D. Haddad et al., "Measurement of the Planck constant at the National Institute of Standards and Technology from 2015 to 2017," *Metrologia*, vol. 54, pp. 633-641, 2017.
[32] B. M. Wood, C. A. Sanchez, R. G. Green, and J. O. Liard, "A summary of the Planck constant determinations using the NRC Kibble balance," *Metrologia*, vol. 54, pp. 399-409, 2017.
[33] S. Schlamminger, and D. Haddad, "The Kibble balance and the kilogram," *Comptes Rendus Physique*, vol. 20, pp. 55-63, 2019.
[34] H. Bettin, K. Fujii, and A. Nicolaus, "Silicon spheres for the future realization of the kilogram and the mole," *Comptes Rendus Physique*, vol. 20, pp. 64-76, 2019.
[35] N. Kuramoto et al., "Realization of the new kilogram using ^{28}Si-enriched spheres and dissemination of mass standards at NMIJ," *MAPAN-Journal of Metrology Society of India*, https://doi.org/10.1007/s12647-020-00393-2, 2020.
[36] D. Raynaud, "Determining the speed of light (1676-1983): An internalist study in the sociology of science," *L´année sociologique*, vol. 63, pp. 359-398, 2013.
[37] K. M. Evenson et al., "Speed of light from direct frequency and wavelength. Measurements of the Methane-stabilized laser," *Phys. Rev. Lett.* Vol. 29, p. 1346, 1972.
[38] T. G. Blaney et al., "Measurement of the speed of light. II. Wavelength measurements and conclusion," *Proceedings of the Royal Society of London. Series A, Mathematical and Physical Sciences*, vol. 355, pp. 89-114, 1977.
[39] P. T. Woods, K. C. Shotton, and W. R. C. Rowley, "Frequency determination of visible laser light by interferometric comparison with upconverted CO2 laser radiation," *Applied Optics*, vol. 17, pp. 1048-1054, 1978.
[40] J. J. Mareš, P. Hubík, V. Špička, J. Stávek, J. Šesták, and J. Krištofík, "Shadows over the speed of light," *Physica Scripta*, vol. 2012, 014080, 2012.